

Short-Term Arctic Cloud Statistics at NSA from the Infrared Cloud Imager

*J. A. Shaw and B. Thurairajah
Department of Electrical and Computer Engineering
Montana State University
Bozeman, Montana*

Introduction

The infrared cloud imager (ICI) is a ground-based infrared thermal imaging system used to identify and classify clouds based on the downwelling atmospheric radiance in the 8-14 μm wavelength region. Data obtained during the ICI's deployment in Barrow, Alaska, in Spring 2002, combined with information provided by radiosondes and microwave radiometers (MWRs), have been used to calculate spatial cloud statistics for the months of March and April 2002. We observe a general trend of increasing cloudiness during this period, and a remarkably short transition time between conditions of clear and cloudy skies.

Infrared Cloud Imager

The ICI comprises an infrared camera using an uncooled micro-bolometer array, a gold-coated beam-steering mirror and a blackbody calibration source, controlled by software that can be accessed remotely (Shaw et al. 2002). The camera records images of the sky at a user-selected interval and relates the downwelling emission in each of 320×240 pixels to the state of cloudiness in that portion of the sky. Before each sky image, ICI performs an internal offset correction to minimize voltage variations across the detector array, and then records an image of an extended-area blackbody source for radiometric calibration.

Figure 1 shows an ICI image from Alaska of a stratus cloud clearing into clear-sky, with a notable cloud edge. ICI images are saved in radiance units, but sometimes displayed, as shown here, color coded in brightness temperature, where blue indicates clear-sky and bright red indicates overcast skies. Intermediate colors indicate clouds of varying optical thickness. The ICI obtains exactly the same measurement in both day and night, unlike visible systems that usually have different operating modes or detection thresholds.

Cloud Statistics

In the 8-14 μm region of the spectrum, the downwelling radiance from a clear atmosphere arises primarily as emission from water vapor (in addition to ozone near 9.6 μm). Thermal emission from clouds causes the radiance in the ICI spectral band to rise above the clear-sky value by a degree that is determined by both the physical cloud temperature and the cloud optical thickness. Generally, thin

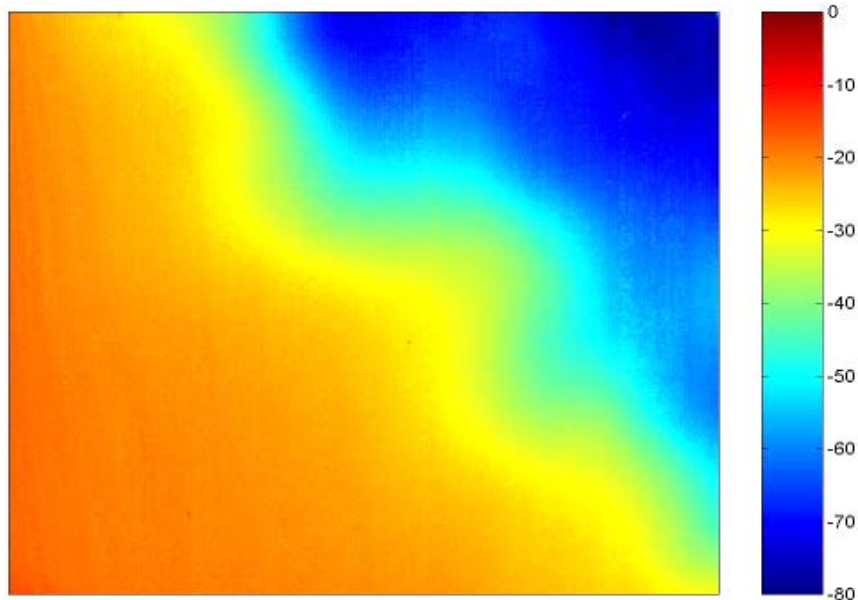


Figure 1. ICI image of clearing stratus clouds.

cirrus contributes a small additional radiance above the clear-sky value, while optically thick liquid clouds (e.g., stratus) generate a much larger radiance value.

Determining cloud statistics from ICI images requires removal of atmospheric water vapor emission, which is highly variable in both space and time (this correction is achieved much more easily when ICI is deployed at an Atmospheric Radiation Measurement (ARM) site because of the full complement of sensors deployed there). We determined a correlation between band-average radiance and total precipitable water vapor from the moderate-resolution atmospheric radiance and transmittance model, which tells us the total water vapor emission. However, not all of the atmospheric water vapor column is below the cloud, which is often sufficiently opaque that the water vapor above the cloud does not contribute to our signal. We have explored several ways of determining the actual water vapor emission arising only from the path below the cloud, but radiative transfer modeling showed that ICI data from Barrow are extremely insensitive to this kind of additional correction. Therefore, for the results shown here, we have simply removed the entire water vapor radiance using the column water vapor measured by the MWR. In future deployments at more humid sites, more detailed water vapor correction will need to be examined (although this is somewhat of a self-correcting problem since cold clouds are usually high enough to be above most of the water vapor, while warm clouds embedded deep within the water vapor layer are very easy to detect and classify with ICI).

If our water vapor correction was perfect, the corrected images would have zero radiance in all pixels for a clear-sky measurement. However, uncertainty in the calibration of the MWR and ICI, as well as variation of water vapor content in space and time, prevents us from achieving this ideal. Nevertheless, we obtain sufficiently small residual radiance values that easily identify all but very thin clouds. We determine a “cloud/no-cloud” threshold using ICI data and simultaneous lidar returns (using the ceilometer and micropulse lidar), and allocate the values nearest zero to a “thin-cloud or uncertain” classification category. Currently we are in the process of examining the sensitivity of ICI to thin cirrus

and the ability of various ICI cloud-identification algorithms to reliably detect these clouds. Cirrus detection with ICI appears to be promising except when the water vapor content is very high.

We used this approach to calculate weekly and monthly cloud statistics for March and April, 2002, which were the only two months of our deployment for which data from all the sensors was sufficiently reliable or available (ICI operated from late January into May at the North Slope of Alaska [NSA] ARM site). The cloud statistics are based on the fraction of cloudy sky radiance in each pixel of the ICI images. The results in Figure 2 show that clear skies prevailed at the end of March, turning to mostly cloudy skies in the first week of April. The intermediate weeks have more nearly equal distributions of clear and cloudy skies, with very short transition periods (in fact, we observe that these short transition times between very cloudy and mostly clear conditions were typical during the period of January-May, 2002 at the NSA site). The last week of April, spreading to early May, again transforms to mostly cloudy conditions. These results, obtained using ICI images with a MWR-based water vapor correction, agree well with the ICI cloud statistics (Figure 3) obtained with a radiosonde-based water vapor correction, although the radiosonde data are limited to only twice a day, whereas MWR data are available much more frequently.

In a study of Arctic cloud characteristics during the Surface Heat Budget of the Arctic Ocean (SHEBA) campaign in 1997-1998, Intrieri et al. (2002) used combined radar and lidar measurements to determine that the monthly-averaged cloud occurrence increased from about 80% in March to almost 90% in April, with mostly cloudy summer months. Monthly cloud statistics from the ICI (Figure 4) also show a general trend of increasing cloudiness from March to April, although the ICI statistics show only about 50% cloudiness in March. The higher percentage of cloudiness at SHEBA may be related to the difference in locations, since our ICI data are from a coastal location (Barrow) and the SHEBA campaign was carried out much farther north, on the frozen Arctic Ocean.

Conclusion and Future Work

This deployment demonstrated the ability of the ICI system to measure cloud statistics in the Arctic, with no difference in threshold or measurement sensitivity between day and night. Long-term deployment of the ICI in the future will pave the way for monthly and yearly spatial cloud statistics and for comparison with other zenith viewing sensors. We are investigating a variety of water vapor correction techniques in the effort to maintain a consistent cloud detection capability, independent of the local water vapor content. The ICI system is deployed from mid-February through mid-April 2003, at the Southern Great Plains (SGP) site in Oklahoma, along with a number of other cloud-statistics sensors as part of the Cloudiness Intercomparison Campaign sponsored by ARM. Future publications will address these issues of data processing and thin-cloud sensitivity. We also anticipate using ICI to study site-diversity statistics for Earth-Space Laser communication, as clouds are a major factor in establishing free-space optical links.

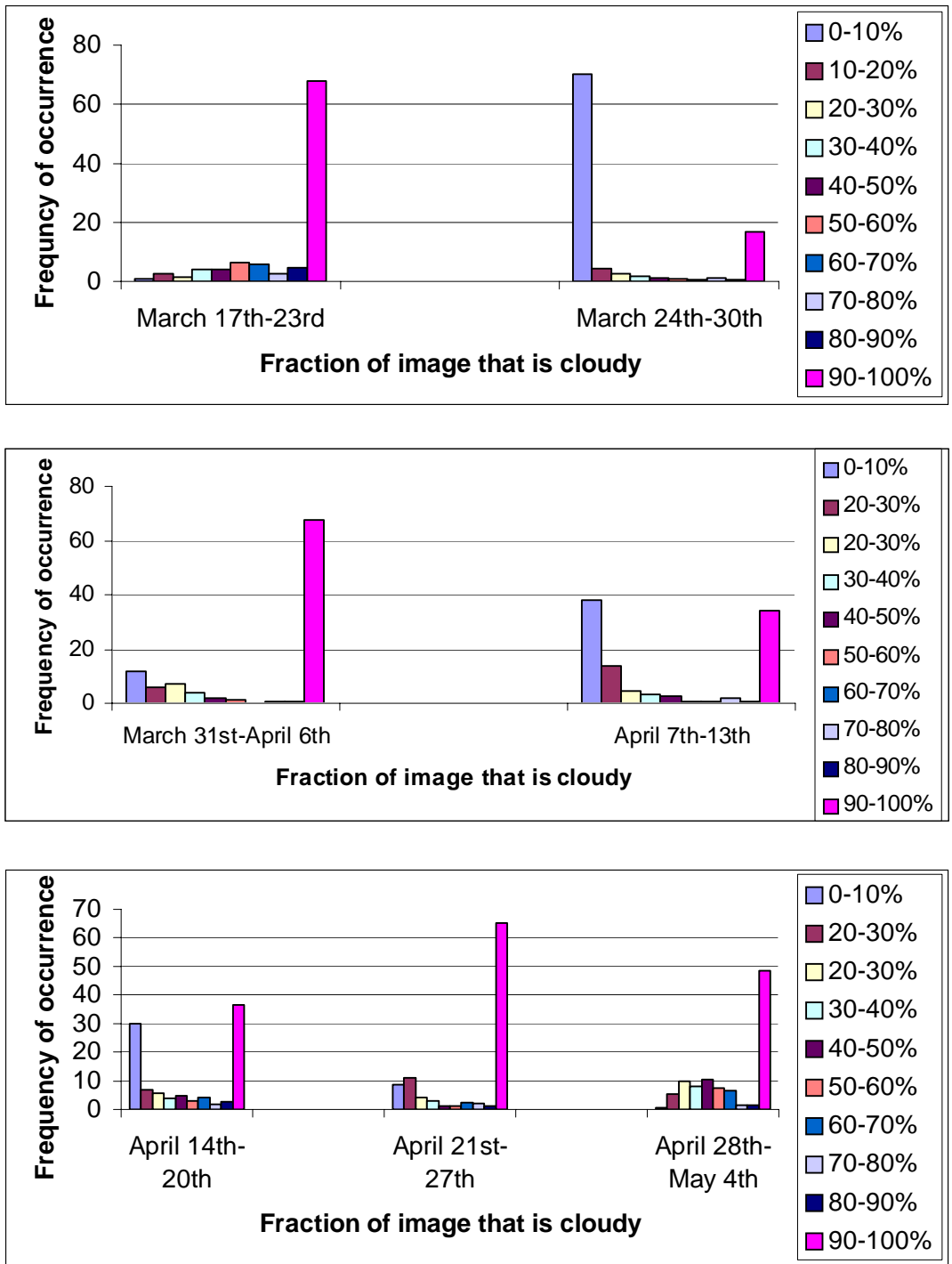


Figure 2. Weekly cloud statistics with data obtained from ICI and MWR.

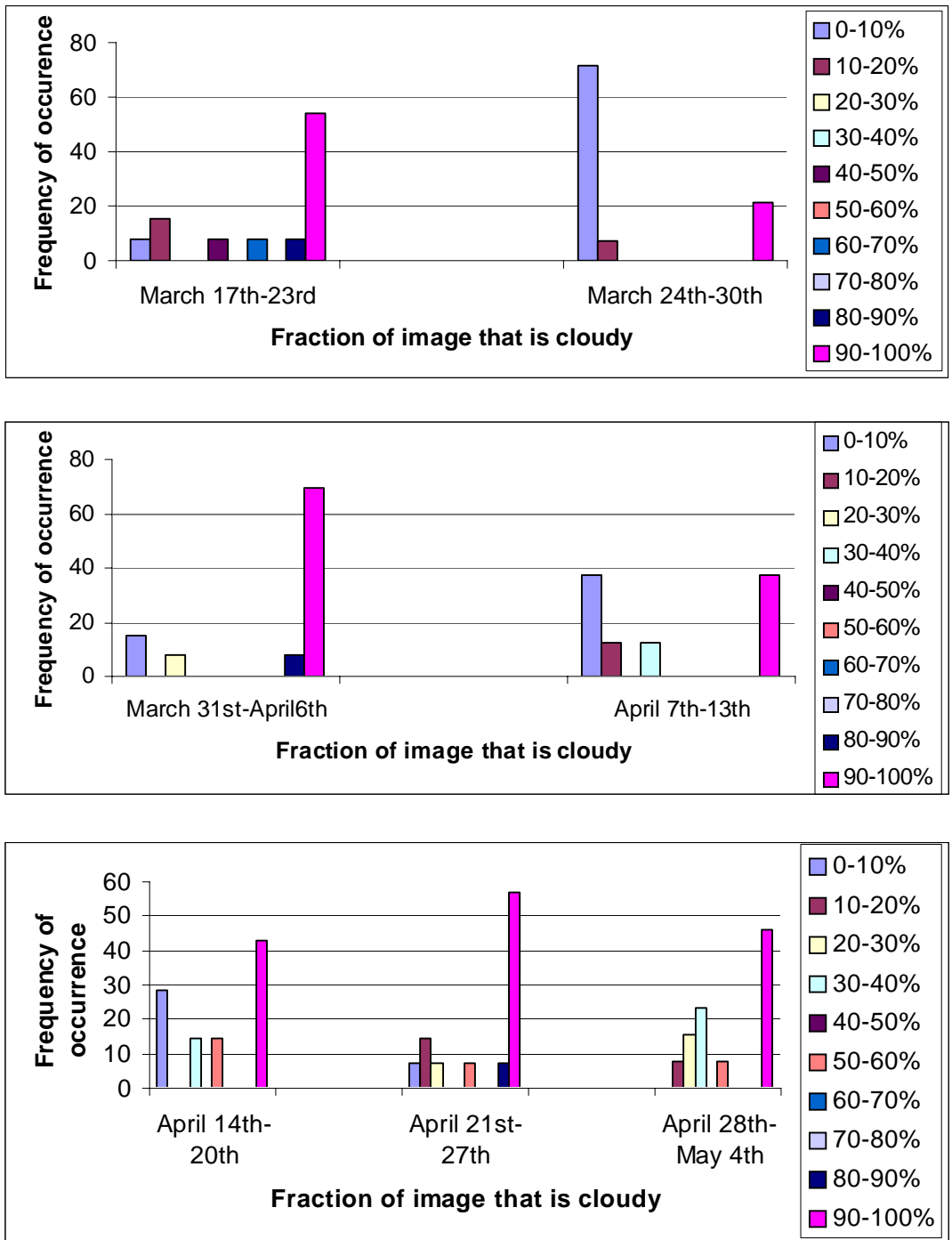
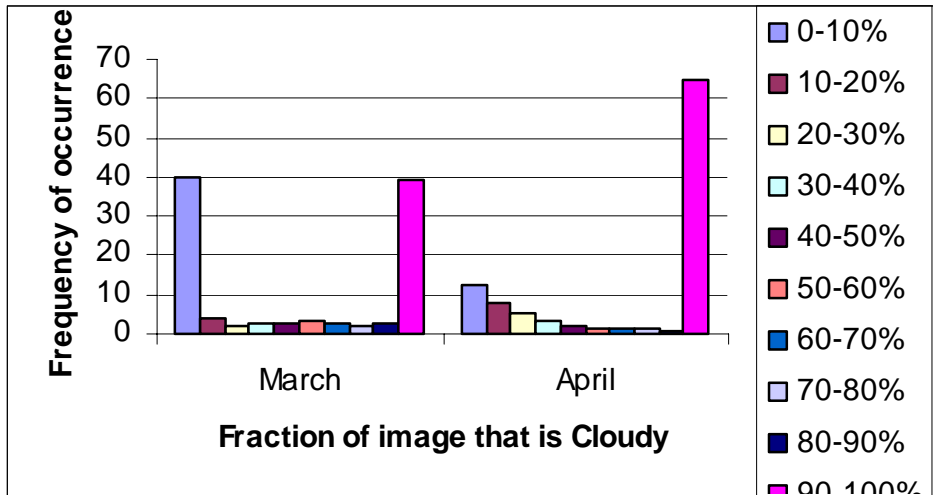


Figure 3. Weekly cloud statistics with data obtained from ICI and radiosonde.

Statistics using ICI and MWR data



Statistics using ICI and Radiosonde data

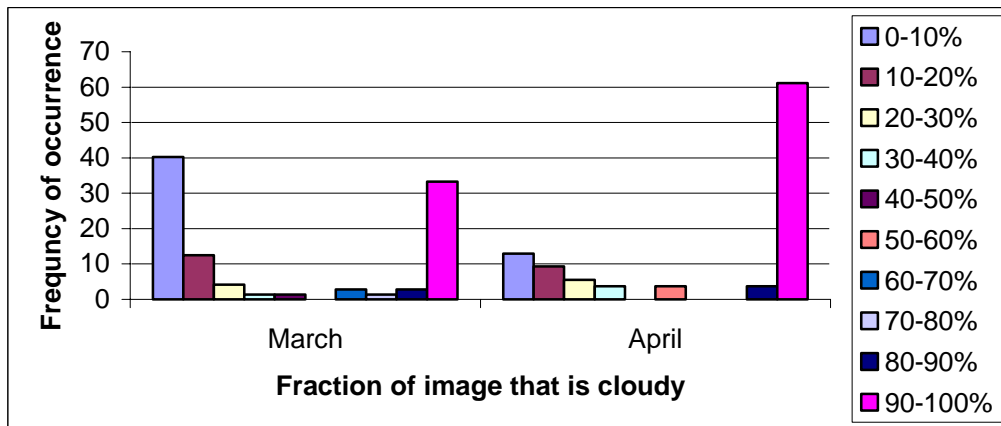


Figure 4. Monthly cloud statistics. (March data limited to the last two weeks)

Acknowledgment

The ICI system was developed by J. A. Shaw and colleagues at the National Oceanic and Atmospheric Administration (NOAA) Environmental Technology Laboratory (ETL) in Boulder, Colorado, with support from the Japanese Communications Research Laboratory (CRL, see www.crl.go.jp). The project moved with J. A. Shaw to Montana State University in late 2001. We gratefully acknowledge the cooperation of CRL through their Arctic atmospheric research program (“Alaska Project”), the contributions of NOAA/ETL employees in the ICI development, the NOAA Arctic Research Office for funding the measurements in Alaska during 2002, and the ARM NSA staff for supporting the ICI deployment.

Corresponding Author

Joseph A. Shaw, jshaw@montana.edu, (406) 994-7261

References

Intrieri, J. M., M. D. Shupe, T. Uttal, and B. J. McCarty, 2002: An annual cycle of Arctic cloud characteristics observed by radar and lidar at SHEBA. *J. Geophys. Res.*, **107**(10), 5-1-5-15.

Shaw, J., A. B. Thurairajah, and E. Edqvist, 2002: Infrared cloud imager deployment at the North Slope of Alaska during spring 2002. In *Proceedings of the Twelfth Atmospheric Radiation Measurement (ARM) Science Team Meeting*, ARM-CONF-2002. U.S. Department of Energy, Washington, D.C. Available URL:

http://www.arm.gov/docs/documents/technical/conf_0204/shaw-ja.pdf